

BACTERIAL BIOPHYSICS

by Andrew Rutenberg

Bacteria are autonomous, robust, ubiquitous, relatively simple, and yet closely related to other living systems. High resolution time-resolved light-microscopy of fluorescently-tagged proteins is enabling the quantitative materials science of these cellular systems. Bacteria are nano-engineers that use proteins as tools; by understanding how they work we can gain important insight into the physics on these small length scales. This paper reviews some progress in developing computational and analytical tools in the study of bacterial biophysics, and some of the exciting directions of this field.

INTRODUCTION

Bacteria, or prokaryotes, are one of the three basic domains of cellular life, along with nucleated eukaryotic cells and the extremophile archaeabacteria. Bacteria comprise millions of species world-wide [1] and are estimated to make up more than half of the world's biomass [2]. Bacteria also represent the earliest life on earth, extending for billions of the 4.5 billion year age of the earth. Early photosynthetic bacteria induced a global transition to an oxygenated atmosphere and so enabled the aerobic lifestyle we enjoy today. Even the energy source of nucleated cells, ATP, is synthesized by endosymbiotic bacteria!

The human genome has approximately 30000 genes. In contrast, an *E. coli* bacterium has only about 4000 genes, and a "minimal" bacterium can survive and reproduce without competition with only about 300 genes [3]. Over 200 complete bacterial genomes have already been sequenced, and are in the process of being qualitatively annotated with the functions of the proteins that they code. The current revolutions in the lifesciences of genomics and proteomics are filling in the biological equivalent of the periodic table of life. Contemporary research in condensed matter physics and materials science depend on the properties of the elements in the atomic periodic table of Mendeleev. For living cells, the emerging list of proteins and their properties make quantitative questions about supramolecular structures and subcellular function compelling to ask and useful to answer.

Bacteria are beautifully rich in their behaviour and function [2]. The book "Molecular Biology of the Cell" [4] describes the exquisite subcellular machinery of both eukaryotic and prokaryotic cells, and the two-volume set

"*Escherichia Coli* and *Salmonella*: cellular and molecular biology" [5] focuses on the detailed mechanisms of these two particularly well-studied bacterial species. What a physicist may find striking about these works is that every page opens new unanswered questions. In particular, quantitative models are still rare. Understanding the physics and materials science of cellular systems will occupy scientists for much of this century.

**Bacteria are nano-engineers
that use proteins as tools;
by understanding how they
work we can gain important
insight into the physics on
these small length-scales.
Moreover, bacteria are
autonomous, robust, ubiq-
uitous, relatively simple,
and yet closely related to
other living systems.**

THE BACTERIAL MACHINE

The standard laboratory workhorse is the intestinal bacterium *E. coli*: a rod-shaped cell approximately 2-4 μm in length and 0.5 μm in diameter. Each bacterium is only 70% water by mass -- the rest is mostly made up of proteins, lipids, and a single looped chromosome of bacterial DNA. The proteins encoded by the bacterial genes have expression levels of up to a few thousand copies each, depending upon their function. The crowded cell interior, or cytoplasm, has a viscosity hundreds of times that of water -- leading to measured diffusivities

for proteins on the order of 1-10 $\mu\text{m}^2/\text{s}$ [6]. This diffusivity is large compared to most length and time-scales of structures within bacteria.

While bacteria lack organelles, such as a nucleus, they do have a dynamically structured interior. A well-fed *E. coli* divides into two "identical" daughter cells every 20 minutes. In addition to molecular synthesis, division requires the orchestration of chromosome segregation, cell-wall synthesis, and the localization of the division midplane. These phenomena utilize a dynamic bacterial cytoskeleton of polymerized filaments consisting of bacterial homologues of actin (MreB) and tubulin (FtsZ) [7], as well as a self-organized standing-wave of Min proteins (see Fig. 1), to accurately subdivide the bacterial length. In contrast to the eukaryotic cytoskeleton, the bacterial cytoskeleton does not appear to have any motor proteins for active transport, any cross-linking between filaments, or any localized organizing bodies such as centrosomes [4]. It may be that these refinements are not necessary in the relatively small and fixed bacterial geometry.

A.D. Rutenberg (andrew.rutenberg@dal.ca), Department of Physics and Atmospheric Science, Dalhousie University, Halifax NS B3H 3J5 (www.physics.dal.ca/~adr).



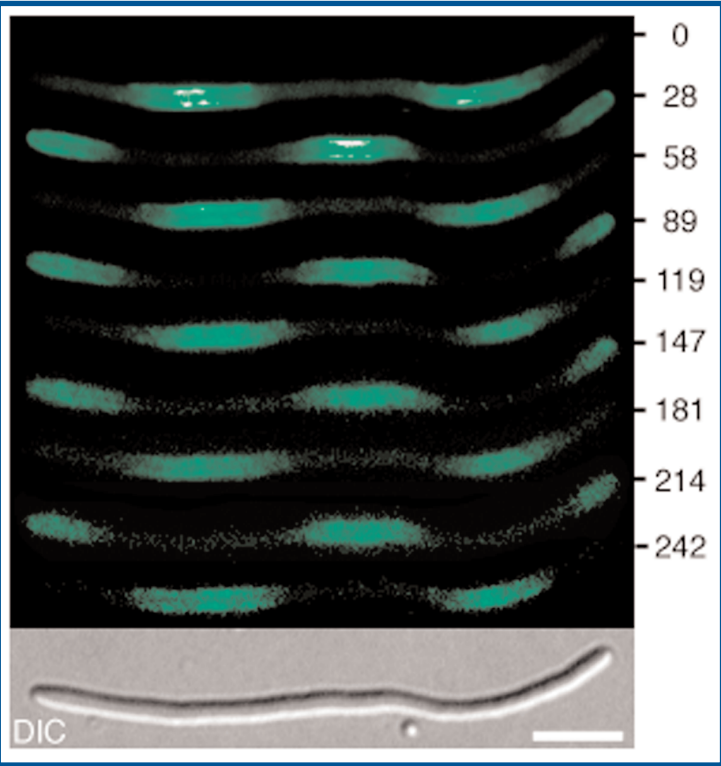


Fig.1 Time-lapse fluorescence micrographs showing the dynamic behaviour of molecules of the fluorescently tagged protein GFP-Mind in a single filamentous *E. coli* bacterium. The protein accumulates on the membrane with a characteristic spacing along the length of the filament, and these maxima oscillate in time^[34, 35]. Time is indicated in seconds along the right side of the figure. The bottom panel shows a non-fluorescent view of the bacterium. The scale bar is 5 mm. [Image courtesy of P. de Boer, Case Western Reserve University.]

The cell wall of a gram-negative bacterium such as *E. coli* is a thin sandwich of a relatively porous outer lipid-membrane, a periplasmic space containing a structural mesh of peptidoglycan (see Boal's paper in this issue), and a tightly regulated inner lipid-membrane. The bacterial outer surface is an active place, with production and shedding of vesicles^[8], constant remodelling during bacterial growth, and trans-membrane export and distribution of surface proteins^[9]. The membrane is also where forces are generated for bacterial motion. Approximately 6 rotational motors traverse the bacterial membrane, and drive *E. coli* forward at speeds of $20 \mu\text{m}/\text{s}$ through the rotation of $20 \mu\text{m}$ long flagellae. Bacteria couple this directed motion to the detection of chemical gradients in "chemotaxis"^[10].

While they can be studied in isolation, bacteria are surprisingly sociable: exchanging genetic material through extendable hollow pili through "lateral gene transfer", exhibiting population-dependent behaviour through "quorum-sensing"^[11], and forming complex macroscopic patterns (see Fig. 2, ^[12]). Bacteria even form simple multi-cellular organisms, with filaments of many genetically identical cyanobacteria differentiating into distinct vegetative or heterocyst cells to survive in Nitrogen depleted environments (see Fig. 3,^[13]). Bacteria are fascinating pattern-forming systems at many length scales, from subcellular to multicellular.



Fig. 2 Chiral patterns formed by a colony of genetically identical *Paenibacillus dendritiformis* bacteria illustrate non-trivial collective effects despite an initially homogeneous and isotropic medium. The chiral pattern is thought to originate from the handedness of the bacterial flagella^[12]. The image is a few cm across. [Image courtesy of E. Ben-Jacob, Tel Aviv University.]

MODERN EXPERIMENTAL TOOLS

To understand dynamic phenomena down to sub-micron scales, the traditional techniques of static high-resolution electron-microscopy, bulk fractionation, and "gels" can only represent starting points. Specialized nanoscale techniques are starting to penetrate microbiology^[14], including the use of AFM (atomic force microscope)^[15], MEMS (micro-electro-mechanical systems) devices^[16], laser tweezers^[17], and microfluidics^[18]. However the largest impact is being made by the pervasive use of time-resolved high-resolution

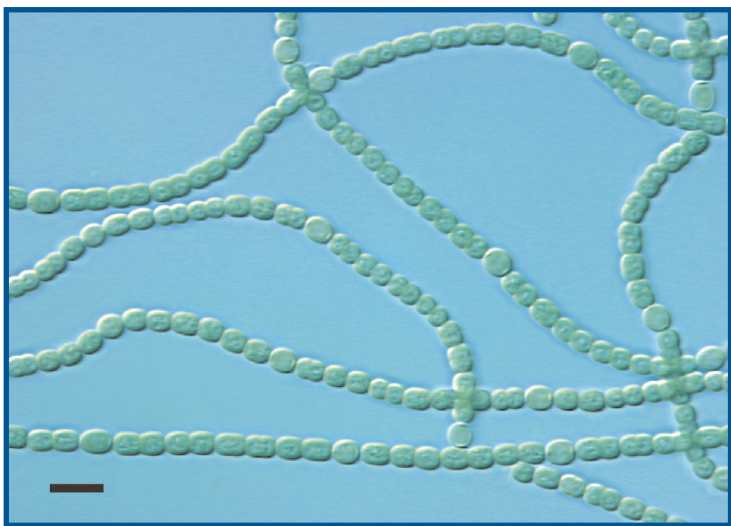


Fig. 3 Filaments of genetically identical *Anabaena* cyanobacteria grown on medium lacking combined nitrogen. The filaments grow as multicellular organisms composed of individual bacteria that have differentiated into one of two cell types: photosynthetic vegetative cells (smaller and dimpled in appearance) and nitrogen-fixing heterocysts (larger and undimpled). During growth, the filaments maintain the pattern of single heterocysts separated by approximately 10 vegetative cells^[13]. The scale bar is 10 microns. [Image courtesy of J. Golden, Texas A&M University.]

fluorescence microscopy. Fluorescent tags can be encoded into the bacterial genome, so that specific proteins are expressed fused to a fluorescent domain (typically GFP, "green fluorescent protein"). Standard light-microscopy can then be used to track the spatio-temporal dynamics of specific proteins within a cell. Advanced optical techniques such as fluctuation spectroscopy and confocal microscopy can also be used.

Researchers are using these techniques to tease out protein mobilities, localization, and interactions within cells (see article by Fradin in this issue). Fluorescence-tagging is also used to track dynamic expression levels of entire genomes from cellular extracts using microarray "gene-chips", such as those commercialized by Affymetrix and Agilent.

The conjunction of so many powerful and reliable quantitative microscopic probes along with increasingly complete lists of bacterial proteins and their functions is raising the standard needed by explanatory models from qualitative to quantitative.

COMPUTATIONAL BIOPHYSICS

Computational biophysics is the computational study of biological systems using the tools of physics. Examples include the study of equilibrium and non-equilibrium aspects of protein folding (see article by Chung in this issue) or of genetic elements such as DNA and RNA (see article by Higgs in this issue). Driven by the information recovered from gene-chip experiments, an emerging computational field is systems biology [18]. Systems biologists model cellular regulatory networks "*in silico*", and pharmaceutical companies hope to use these models to systematically identify good drug targets and improve the resulting drugs.

However, cells are not simply bags of proteins. To understand cellular function in detail we will need to supplement a systems biology of genomic and biochemical networks with an understanding of the self-assembly and regulation of subcellular structures. A quantitative understanding of how subcellular structures affect protein interactions will be essential to accurately model whole cells. Understanding the self-organized structures and emergent functions of collections of proteins within cells will provide us with the design constraints and blueprints of cellular function. Mature quantitative models could also be used to relate observable behaviour with microscopic interactions in order to extract biochemical interactions *in vivo*, and to use bacteria as quantitative probes of their environment. To fully realize this vision we will have to understand the collective or materials properties of many independent structures

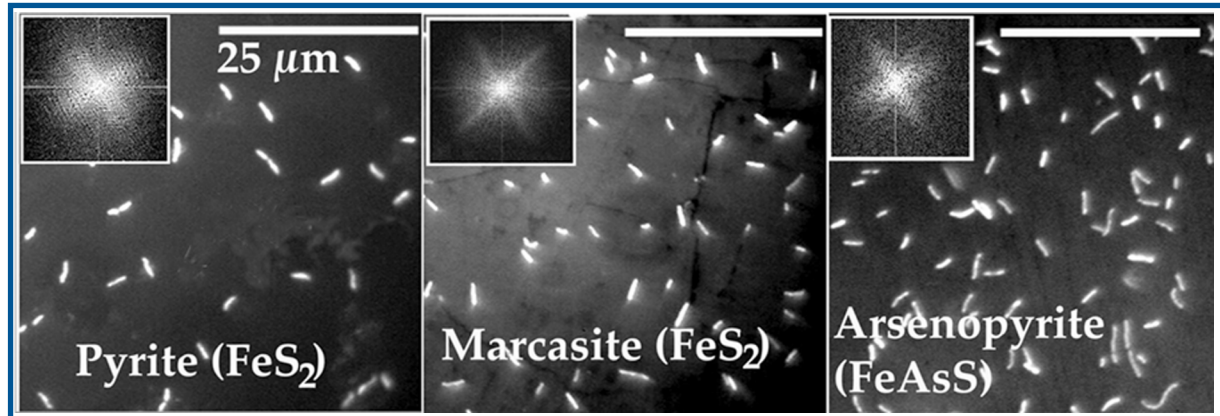


Fig. 4 Bacterial cells attached to oriented metal sulfide minerals. Insets show Fourier transforms for each region, illustrating the directions of preferential cell alignment along crystalline directions [20]. The scale-bar is the same for all three images. [Image courtesy of K. Edwards, Woods Hole Oceanographic Institution.]

within and around bacteria, and then knit them together. This is the focus of our work in computational bacterial biophysics, and some of the problems we have modeled will illustrate this growing field with respect to bacterial adhesion, motility, and division.

BACTERIAL ADHESION

Many bacteria in the environment attach to mineral surfaces and affect mineral dissolution and precipitation [19]. Understanding what influences the initial adhesion of bacteria to mineral substrates can help us understand biological weathering and corrosion processes. In some crystalline samples, bacteria align with *no* visible surface features, though parallel to the crystallographic orientation (Fig. 4). We have investigated [20] how the microtopography of a substrate could influence the initial reversible attachment of bacteria, before irreversible attachment is achieved through the production of polysaccharides, pili, fibrils, and other bridging appendages. There needs to be a significant energy difference associated with surface microtopography, compared to the thermal energy $k_B T$, for cell alignment to be biased.

Reversible Adhesion

Interaction strengths can be estimated from optical tweezer experiments that measure interactions between a single bacterium and a flat glass plate [21]. They measure forces ranging from $10^{-14} N$ to $10^{-12} N$ with a range of 10 nm. Flow experiments achieve desorption with similar forces [22]. This corresponds to a binding energy of a few $k_B T$, which is consistent with the routine observation of spontaneous desorption. For a typical Gram-negative acidophile, such as *Thiobacillus caldus*, with no visible extracellular coat, we find that elastic deformations are of high energy and should not contribute significantly to adhesion [20]. Consequently, we quantitatively model a fixed geometry bacterium. We approximate the interaction by an exponential with a local interaction strength of $V_O = 27 k_B T/\mu m^2$, corresponding to a total binding energy of $\sim 5 k_B T$, and allow it to exponentially decay away from the surface with decay length $\eta = 15 \text{ nm}$ [23]. Our results are qualitatively insensitive to these details.

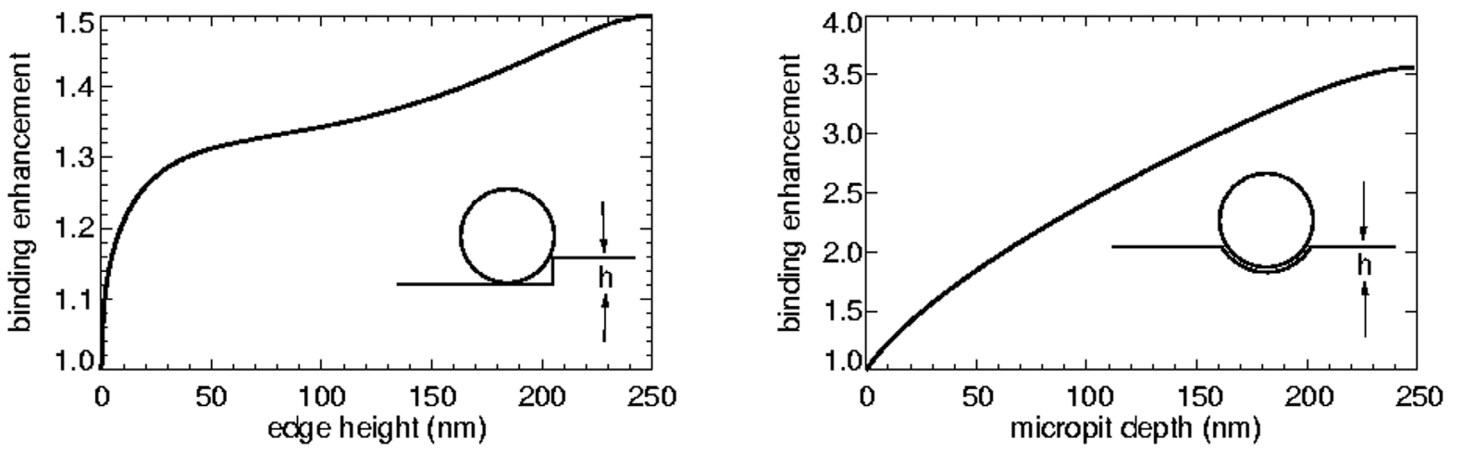


Fig. 5 (a) The enhancement factor of the binding strength for a bacterium resting against a step-edge plotted against the step-edge height h . (b) The enhancement factor for a bacterium nestled in a small cylindrical micropit vs. the micropit depth, h (note the vertical scale difference). In both bases significant binding enhancement is seen for relatively small features.

Bacterial-shaped depressions can significantly affect the bacterial binding strength, and we have calculated the binding enhancement for "U" shaped grooves of the bacterial radius and varying depths, see Fig. 5. We see that depressions of depth 10 nm can lead to a noticeable binding enhancement for the bacterium. Independent of alignment issues, this is a mechanism for significantly enhancing bacterial adhesion and localization. This suggests that over quite short time scales strong reversible adhesion could result from local alterations in the surface microtopography due to microbial metabolism. Another possible mechanism for alignment is from isolated step-edges due to oxidation fronts on the pyrite surface. The enhancement factor compared to the binding to a flat substrate is shown in Fig. 5 with respect to the step height in nm. A significant enhancement is also seen with a 10 nm step edge.

Optically-invisible crystallographically-aligned surface features could cause the bacterial alignments shown in Fig 4, and so we are not forced to evoke baroque biological mechanisms to explain the alignment. To confirm this simple picture, experimental studies are now underway to better characterize bacterial etch-pits, their alignment, and their evolution. While the large oriented surfaces of Fig. 4 are not common naturally, they do serve as ideal substrates to better understand the detailed adhesion mechanisms of bacteria on natural minerals. Since bacterially mediated mineral dynamics may have a large geological impact over planetary timescales, and a large environmental impact over human timescales through acidified mine tailings, understanding bacterial adhesion and subsequent etching at the microscopic scale is important.

BACTERIAL MOTILITY

Pathogenic bacteria that invade and infect host cells are sometimes able to hijack the host cell proteins for their own advantage [24]. Such bacteria can be used as easily visible probes into the mechanisms of the host-cell, and once the mechanisms are well-characterized, as assays of the host-cell conditions. As an example, curved "comet-tails" of poly-

merized host-cell actin push the pathogenic bacterium *Listeria monocytogenes* through the cytoplasm of a host eukaryotic cell. Similar actin tails are associated with *Shigella flexneri*, spotted-fever *Rickettsiae*, the *Vaccinia* virus, and even host-cell vesicles [25]. The force generated by actin polymerization drives the particle forward against the viscous drag of the cytoplasm in a fluctuation-ratchet mechanism [26]. The only bacterial contribution to motility is a single surface protein that locally promotes the nucleation, elongation, and cross-linking of actin filaments. As the bacterium or particle moves forward within the cell, a curved comet-like tail of actin filaments remains behind as a record of the trajectory. We have studied this curvature, which is fundamentally a fluctuation effect [27, 28].

Curved Trajectories

Curved trajectories imply that in addition to a net force F pushing the bacterium forward against viscous drag, there must be a torque N acting on the bacterium. We can use the drag coefficients for a hemispherically capped cylinder of length a and radius b [29] to obtain the curvature $K = 3N / [2(a^2 + b^2) F]$ independent of the viscosity. We find that the curvature directly probes the ratio of force and torque applied to the bacterium by the polymerizing actin filaments.

If there are n actively pushing filaments, then the force $F = f_0 n$ is proportional to the force per filament f_0 , which in turn will depend on the microscopic details of force generation. If the filaments are randomly placed on the trailing end of the bacterium, each one will produce a random vectorial torque on the bacterium. The sum of many random torques will have a Gaussian distribution with zero mean. Uniformly distributing the filaments over the hemispherical bacterial endcap with density σ leads to an RMS torque

$$N_{RMS} = \sqrt{\langle N^2 \rangle} = f_0 b^2 \sqrt{4\pi\sigma/3}$$

so that

$$K_{RMS} = \frac{b\sqrt{3}}{(a^2 + b^2)\sqrt{2n}} \quad (1)$$

This result is independent of the details of the force generation mechanism. Observed curvatures are consistent with the number of filaments seen in electron microscopy [27]. This illustrates how a relatively simple model can be used to extract nanometer scale structure that is not resolved by light-microscopy, the number of filaments n , from the visible shape of the bacterium and its trajectory.

Curvature Dynamics

Individual bacteria do not go in simple circles even in homogeneous cellular extracts. How can we understand the change of curvature from one moment to the next? We consider the autocorrelation of the vector torques

$$A(\Delta t) \equiv \langle \mathbf{N}(t) \cdot \mathbf{N}(t + \Delta t) \rangle = N_{RMS}^2 e^{-\Delta t/\tau} \quad (2)$$

where circular motion corresponds to $\tau = \infty$. The general form of the autocorrelation decay follows directly if each filament has a lifetime τ after which it is replaced randomly on the rear of the bacterium by another filament. If new filaments are randomly placed, their torques will be uncorrelated with those from other filaments. The autocorrelation will then be proportional to the fraction of filaments that have not been replaced between the two times, *i.e.* $e^{-(t_2-t_1)/\tau}$. Exponential decay also applies for actin filaments whose fast-growing barbed-end positions diffuse over the bacterial surface with diffusion constant D , where we find $\tau = b^2 / (2 D)$ [27].

For individual bacteria tracked for times much less than τ , the curvature will appear constant. For times much longer than τ , each bacterium will sample the ensemble of curvatures. The autocorrelation decay of the curvatures will then characterize filament replacement and/or diffusion at the bacterial surface. We can thereby extract microscopic dynamical information about filament turnover that is not accessible by either time-resolved but relatively low-resolution light-microscopy or static but high-resolution electron microscopy. More sophisticated models, in conjunction with experimental observations such as bacterial rotations about their long-axis [30], should lead to more detailed probes of the structure and dynamics of the actin tail behind moving intracellular bacteria and vesicles.

Vesicle Diffusion

Biological systems can also inspire fundamental physics research. Motivated by the changing curvatures of intracellular particles we have just discussed, we have char-

acterized the diffusivity of particles with constant speed but changing curvatures [28]. We examine both a "broken swimmer" with a fixed curvature magnitude but with an axis of curvature that is reoriented by fluctuations (rotating curvature, RC), and a "microscopic swimmer" with a normally-distributed curvature that is spontaneously generated by fluctuations (Gaussian curvature, GC). In both of these systems, the changing curvature leads to particle diffusion at long times.

Particles moving at a constant speed will change direction via $\partial_t \mathbf{v} = -\mathbf{v} \times \mathbf{K}$, where \mathbf{K} is the vector curvature. For "rotating curvature" dynamics (RC) the curvature magnitude is constant, $|\mathbf{K}| = K_0$, but the curvature randomly rotates around the direction of motion so that

$$\partial_t \mathbf{K}_{RC} = \xi \hat{\mathbf{v}} \times \mathbf{K} \quad (3)$$

where the Gaussian noise ξ has zero mean but $\langle \xi(t) \xi(t') \rangle = 2\delta(t-t')/\tau$ with a characteristic timescale τ . For "Gaussian curvature" dynamics (GC) the curvature magnitude changes through

$$\partial_t \mathbf{K}_{GC} = -\mathbf{K}/\tau + \xi \quad (4)$$

where the Gaussian noise ξ is perpendicular to \mathbf{v} with zero mean and $\langle \xi(t) \cdot \xi(t') \rangle = \delta(t-t')K_0^2/\tau$. The resulting curvatures are Gaussian distributed in each component. We show typical trajectories for RC and GC dynamics in Fig. 6.

The diffusivity of a particle is given by $D \equiv \langle r^2 \rangle / (2dt)$ in the limit as the elapsed time $t \rightarrow \infty$ in spatial dimension d . We use computer simulations to measure the diffusivity of these systems as a function of the root-mean-squared curvature K_0 , the constant particle speed v , and the timescale characterizing the curvature dynamics τ . Dimensional analysis shows that there is only one free parameter in the problem, and we show the dimensionless diffusivity vs. the dimensionless speed for $d=3$ in Fig. 7, where the dimensionless diffusivity is

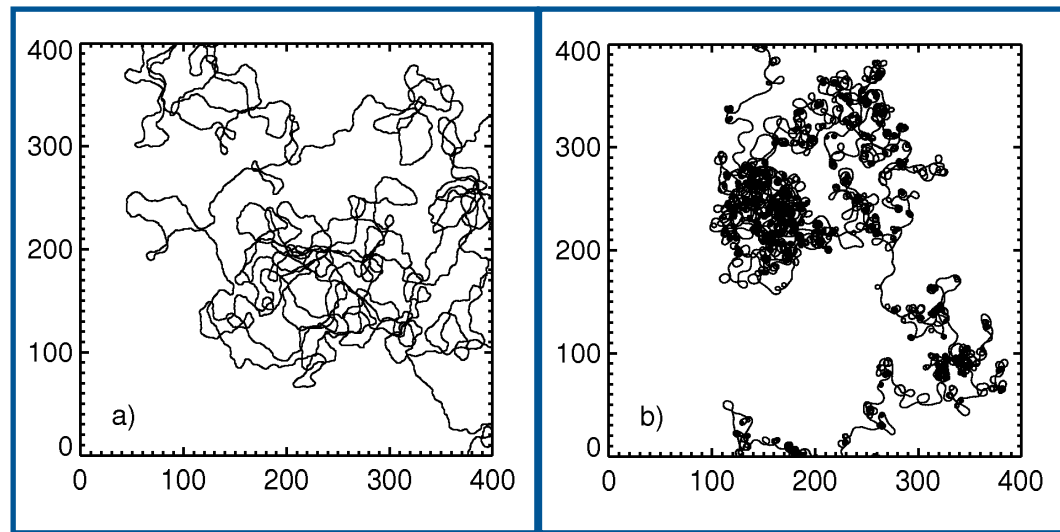


Fig. 6 (a) Typical particle trajectory with dynamic Gaussian curvature (GC) with $v^*=0.1$. The particle does not complete a circular loop before K changes significantly. (b) Here, $v^*=100$. The particle can complete many circular loops before K changes; however straight segments are seen when $|K|$ is small. The result is a characteristic "knotty wool" appearance. In both cases $K_0=1$.

$$D^* \equiv DK_0^2\tau \quad (5)$$

and the dimensionless speed is

$$v^* \equiv vK_0\tau \quad (6)$$

Can we qualitatively understand the asymptotic behaviour of D^* ? For RC dynamics the instantaneous curvature does not change in magnitude even while the curvature axis wanders. The particle will go in a circular trajectory, not contributing to diffusivity, until the curvature axis wanders significantly. The result is a random walk with step size given by the radius of curvature $\Delta r \sim 1/K_0$ and an interval between steps of τ , leading to $D \sim 1/(K_0^2\tau)$ or $D^* \sim \text{const}$. In fact, an exact analogy between the curved trajectory and the static configuration of a hindered jointed polymer chain [31,28] confirms $D^* = 1/3$, and agrees precisely with the simulations.

For a GC trajectory in $d=3$, there is no obvious polymer analogy since the curvature magnitude as well as its direction evolves with time. In the limit of $\tau \rightarrow 0$ however, the curvature is independently distributed at every point along the trajectory and the diffusivity can be extracted from the "worm-like chain" polymer model originally solved by Kratky and Porod [32]. The result is again $D^* = 1/3$, but only for small v^* . It is more difficult to understand the $D^* \sim (v^*)^\lambda$ behaviour for large v^* . Indeed, the exponent $\lambda = 0.71 \pm 0.01$ represents a qualitatively new type of diffusive behaviour.

It is interesting to compare diffusion of curved swimmers to passive thermal diffusion, characterized by $D_T = k_B T / (6\pi\eta R)$. Within the context of actin-polymerization based motility of small intracellular particles, for a given surface-density of filaments we obtain $K_0 \sim A/R^2$ from Eq. 1, so that larger particles will follow straighter trajectories. Using Eq. 5 and 6 with the results of Fig. 7, we see that D increases with increasing particle size for all particle speeds! This is in dramatic contrast with thermal diffusion, where diffusivities always decrease with particle sizes. For actin-polymerization based motility, we find [27] that for all sizes above $R_c \approx 80 \text{ nm}$ a particle will have a higher diffusivity by actively swimming by the actin-polymerization mechanism than by passive thermal diffusion. This provocatively lies close to typical vesicle sizes seen within eukaryotic cells. Indeed, this motility mechanism is observed for vesicles that are not moving along pre-existing cytoskeletal tracks [25]. Our results in Fig. 7 can be used to relate microscopic dynamical information such as the time-scale of curvature dynamics τ , or the vesicle speed v , to the RMS curvature K_0 and the bulk diffusivity D . This provides another example of quantitative models linking macroscopic phenomena that are relatively easy to experimentally characterize with microscopic phenomena that are not.

BACTERIAL DIVISION

Each *E. coli* cell divides roughly every hour, depending on conditions -- first replicating its DNA into two separate nucleoids, and then dividing at midcell into two daughter cells. If the division apparatus does not assemble accurately at midcell then DNA will not be distributed to both daugh-

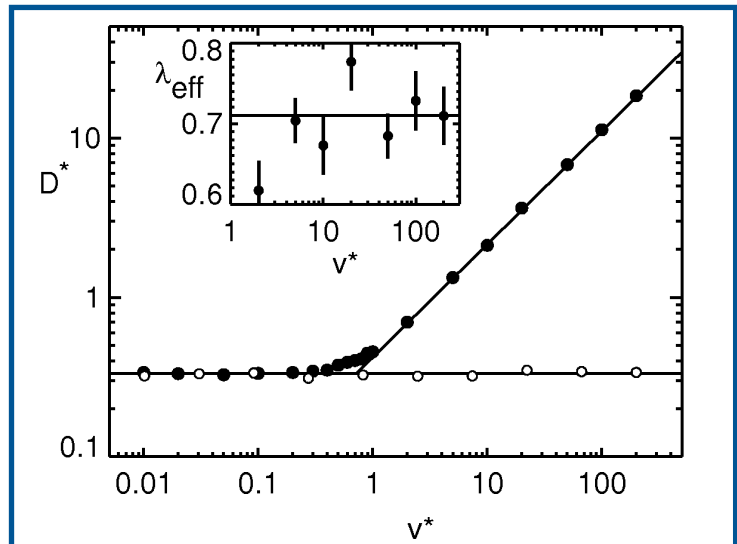


Fig. 7 Dimensionless diffusivities $D^* = DK_0^2\tau$ for fixed magnitude curvature (open circles, RC) and Gaussian-distributed curvature (filled circles, GC) dynamics in $d=3$, plotted against dimensionless particle speed $v^* \equiv vK_0\tau$. Solid lines show the exact result $D_{RC}^* = 1/3$, as well as the large v^* power-law asymptote $D_{GC}^* \sim (v^*)^\lambda$. The inset shows effective exponents between sequential points, for Gaussian curvatures, with a solid line indicating the best-fit $\lambda = 0.71$.

ter cells, resulting in unviable anucleate "minicells". Division is initiated by a polymerized ring of the protein FtsZ, which forms on the inside of the bacterial membrane. Precise positioning of the FtsZ ring is controlled by the MinCDE system of proteins [33]. MinC inhibits the formation of the FtsZ ring, and is recruited to the membrane by MinD. MinE is also recruited to the membrane by MinD, but it then locally releases the MinD and MinC from the membrane and allows the FtsZ ring to form. A remarkable oscillatory dynamics is seen [34,36,37], as illustrated for MinD in Fig. 1. First the MinC/MinD accumulate at one end of the bacterium on the cytoplasmic membrane. Then MinE forms a band at midcell which sweeps towards the cell pole occupied by the MinC/MinD, ejecting the MinC/MinD into the cytoplasm as it goes. The ejected MinC/MinD then rebinds at the other end of the bacterium. When the MinE band reaches the cell pole, it disassociates and reforms at midcell. The entire process then repeats towards the opposite cell pole. The oscillation period is approximately one minute, so many oscillations occur between each bacterial division. The dynamics minimizes the MinC/MinD concentration at midcell of short bacteria, thereby allowing the FtsZ-ring and the subsequent division septum to form only there.

To model this phenomenon we use a set of four coupled reaction-diffusion equations describing the densities of MinD on the cytoplasmic membrane (ρ_d), MinD in the cytoplasm (ρ_D), MinE on the cytoplasmic membrane (ρ_e), and MinE in the cytoplasm (ρ_E) [38]. We do not model the MinC field explicitly since MinC simply tracks the MinD density [36]. We consider the variation of densities along the long bacterial axis, with dynamics coming from diffusion and from transfer between the cytoplasmic membrane and the cytoplasm:

$$\begin{aligned} \frac{\partial \rho_D}{\partial t} &= D_D \frac{\partial^2 \rho_D}{\partial x^2} - \frac{\sigma_1 \rho_D}{1 + \sigma'_1 \rho_e} + \sigma_2 \rho_e \rho_d \\ \frac{\partial \rho_d}{\partial t} &= \quad \quad \quad + \frac{\sigma_1 \rho_D}{1 + \sigma'_1 \rho_e} - \sigma_2 \rho_e \rho_d \\ \frac{\partial \rho_E}{\partial t} &= D_E \frac{\partial^2 \rho_E}{\partial x^2} - \sigma_3 \rho_D \rho_E + \frac{\sigma_4 \rho_e}{1 + \sigma'_4 \rho_D} \\ \frac{\partial \rho_e}{\partial t} &= \quad \quad \quad + \sigma_3 \rho_D \rho_E - \frac{\sigma_4 \rho_e}{1 + \sigma'_4 \rho_D} \end{aligned} \quad (8)$$

The total amount of MinD or MinE has been explicitly conserved in our dynamics since oscillations persist without protein synthesis [34].

We see in Fig. 8 that the oscillating pattern spontaneously generates itself from a nearly homogeneous initial condition, reflecting a linear instability. Nonlinearities stabilize the eventual oscillating state. At the midcell, the oscillating pattern has a minimum of the time-averaged MinD concen-

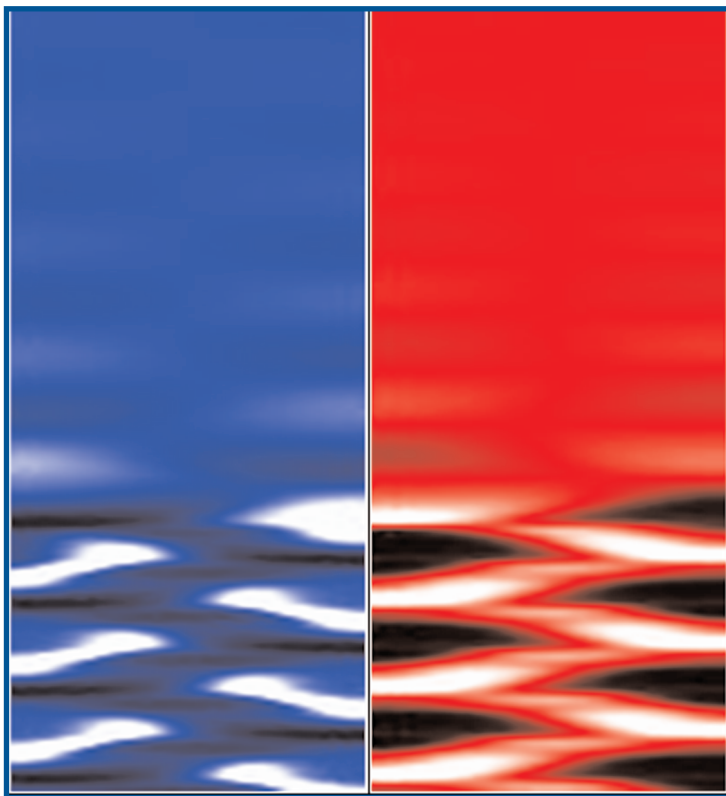


Fig. 8 Space-time plots of the total MinD (left, blue) and MinE (right, red) densities for the model described by Eqns. (8). The brightness scale runs from 0.0 (black) to 2.0 (white) times the average density of MinD or MinE. Time increases from top to bottom (total time from top to bottom is 18 minutes). The configuration has been started from a nearly homogeneous state with a small amount of white noise, and through a linear instability it evolves into the oscillating pattern which then repeats indefinitely as time continues. The MinD depletion from mid-cell is immediately evident. The horizontal scale spans the 2 micron bacterial length. [Image courtesy of S.de Vet.]

tration --- an essential feature for division regulation. We have also investigated longer filamentous bacteria and found multiple MinD and MinE bands, consistent with the filamentous *E. coli* shown in Fig. 1. The characteristic wavelength is reassuringly longer than a normal *E. coli* bacterium just before division. A shorter wavelength would mean that multiple MinD bands would occur in bacteria of normal lengths and division would not always be at the midcell.

Stochastic Model

Bacterial proteins are typically present in low numbers within the cell. In *E. coli*, a recent assay found only a couple of thousand molecules of MinD or MinE per cell [39]. We have investigated the role of fluctuations in a discrete particle model where each protein molecule is explicitly tracked [40]. In this way, the full fluctuation effects of shot-noise are intrinsically included in our model. For different number of Min molecules, N , we have scaled our interaction parameters so that they lead to the same deterministic behaviour. This allows us to investigate the effects of various levels of shot-noise. We find that the midcell MinD concentration minimum is still robustly reproduced even in the presence of noise. However the fluctuations around this average can be very large for small N . In Fig. 9 we show histograms of the position of the MinD concentration minimum, where each minimum is determined over a single oscillation cycle.

Assuming that FtsZ nucleation occurs at a single cycle MinD minimum, then from Fig. 9 we see that $N=1500$ is a high

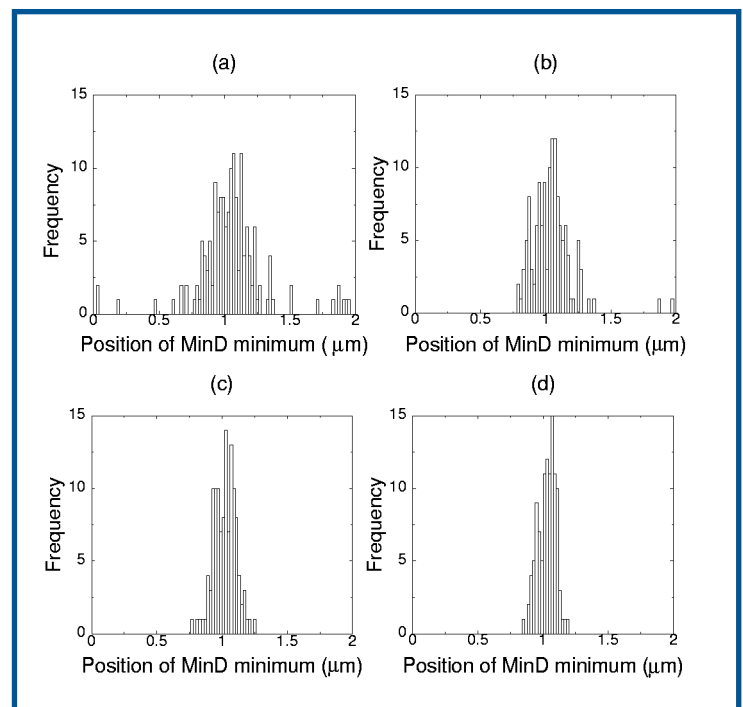


Fig. 9 Histogram of the location of the MinD density minimum, averaged over a single oscillation cycle, in a discrete-particle simulation of Eqns. (8) with identical deterministic dynamics but varied particle numbers: (a) $N=200$, (b) $N=400$, (c) $N=800$, (d) $N=1500$. The midcell minimum is only robustly identified with close to natural expression levels ($N \sim 1000$), indicating that bacteria may select expression levels to minimize stochastic effects in this system.

enough expression level to reduce the probability of polar division to considerably less than 0.01 per oscillation cycle. Given that about 50 complete oscillation cycles normally occur between successive divisions, attaining this level of accuracy is important. Lower expression levels than $N=1500$ lead to a significant probability of polar division, while larger N will only marginally improve division accuracy and at the cost of manufacturing more protein.

Experimentally, the precision of the Min system can be probed in anucleate cells by measuring the position of the FtsZ ring. In these cells the FtsZ ring position is placed at midcell within a range of $0.12 \mu\text{m}$ [41], quite similar to the MinD distribution width $0.07 \mu\text{m}$ we see at $N=1500$. *E. coli* appears to use just enough Min protein to mitigate the effects of shot-noise.

FUTURE DIRECTIONS

There are some important challenges in the field of computational biophysics. I will illustrate some of these in the context of the Min system of midpoint determination in *E. coli*. There are currently four competing reaction-diffusion models for Min oscillation [38,42], and they each have from 7 to 17 microscopic parameters. Experiment has not yet measured any of those parameters directly. How can experiment falsify a 10 parameter model with anything but direct measurement of those parameters? Complicating this challenge is that there is much qualitative phenomenology that has not yet been included in any model. For example, filamentous structures in *E. coli* [43] are either passively decorated by oscillating Min proteins, and so are appropriately excluded, or are actively involved in the oscillation, and so must be included. One approach that may work is to impose the property of "robustness" [44] to model systems. However it is still an open question of how robustness in specific systems can be exploited to predict microscopic parameters.

Stochastic effects may prove to be useful in this regard, since models must work in the presence of intrinsic shot-noise and must reproduce experimental signatures of stochastic effects without any additional free parameters. We are the only group so far to explore the effects of shot-noise in Min oscillation [40]. However there remain significant computational challenges in modelling stochastic partial differential equations in general biological systems [45].

Appropriating the lessons Steven Weinberg learned from particle physics in the 1960s: biophysics is an area where creative work can still be done; it is where the action is. There are tremendous opportunities for people with the quantitative training and mindset of physics, who are open to and curious about quantitatively charting and modelling the waters of biology. The study of bacteria is an ideal place to begin.

RESEARCH IN BACTERIAL BIOPHYSICS

There are a great many specific open questions in bacterial biophysics! There is no better way of being exposed to these open puzzles than by speaking with the experimentalists who are giving them form. I can recommend attending biological meetings, such as Gordon Conferences or ASM conferences (American Society of Microbiology). For stu-

dents, the best way to explore a field is to work in it. Great progress is often made by scientists who switch fields and the history of biology is punctuated by important work being done by biologists who started in other sciences. Switching disciplines is not necessary though: a number of physicists study bacteria. I list here some names of physicists worldwide who are working in bacterial biophysics: their papers and/or their groups can provide good starting points for further exploration.

Some notable efforts internationally include:

- France: Jacques Prost (Institut Curie)
- Germany: Alexei Boulbitch (Munich)
- Israel: Uri Alon (Weizmann)
- Eshel Ben-Jacob (Tel Aviv)
- Japan: Mitsugu Matsushita (Chuo Univ.)
- UK: Martin Howard (Imperial)
- USA: Bob Austin (Princeton)
- Howard Berg (Harvard)
- Philippe Cluzel (Chicago)
- Michael Elowitz (CalTech)
- John Kessler (Arizona)
- Stan Leibler (Rockefeller)
- Albert Libchaber (Rockefeller)
- George Oster (Berkeley)
- Alexander van Oudenaarden (MIT)

Canada is well represented in this field, with research efforts underway across the country including:

- David Boal (SFU): bacterial architecture
- John Dutcher (Guelph): bacterial biofilms
- Manfred Jericho (Dalhousie): AFM studies of bacteria
- David Pink (StFX): modelling bacterial surfaces
- Andrew Rutenberg (Dalhousie): modelling of bacteria
- Gary Slater (Ottawa): modelling biofilms
- Jack Tuszyński (Alberta): "Project Cybercell"

ACKNOWLEDGEMENTS

We acknowledge stimulating collaborations with K. Edwards, M. Howard, M. Grant, S. de Vet, A. Richardson, and C. Montgomery. We also acknowledge valuable discussions with J. Theriot, P. de Boer, T. Lutkenhaus, and M. Jericho. We are grateful for the wonderful experimental images provided by E. Ben-Jacob, P. de Boer, K. Edwards, and J. Golden. This work was supported by NSERC under GSC28.

REFERENCES:

1. T.P. Curtis *et al.*, "Estimating prokaryotic diversity and its limits", *PNAS*, **99**:10494-10499 (2002).
2. For a general introduction to bacterial metabolism and habitats see J. Postgate, *The Outer Reaches of Life*, Cambridge University Press, 1994. For a popular introduction to subcellular processes see F. M. Harold, *The Way of the Cell*, Oxford University Press, 2001.
3. C.A. Hutchison *et al.*, "Global transposon mutagenesis and a minimal Mycoplasma genome", *Science*, **286**:2089-2080 (1999).
4. B. Alberts *et al.*, *Molecular Biology of the Cell*, 4th Ed, Garland Science, 2002.
5. *Escherichia Coli and Salmonella: Cellular and Molecular Biology*, 2nd ed, eds. F.C. Neidhardt, R. Curtiss, and E.C. Lin, ASM Press, 1996.

6. M. B. Elowitz *et al.*, "Protein mobility in the cytoplasm of *Escherichia coli*", *J. Bacteriol.*, **181**:197-203 (1999).
7. R. Carballido-López and J. Errington, "A dynamic bacterial cytoskeleton", *Trends in Cell Biology*, **13**:577-583 (2003).
8. T.J. Beveridge, "Structures of gram-negative cell walls and their derived membrane vesicles", *J. Bact.*, **181**:4725-4733 (1999).
9. J.R. Robbins *et al.*, "The making of a gradient: IcsA (VirG) polarity in *Shigella flexneri*", *Mol. Microbiol.*, **41**:861-872 (2001).
10. H. Berg, "Motile Behavior of Bacteria", *Physics Today*, **53**:21-29 (2000).
11. S. Park *et al.*, "Influence of topology on bacterial social interaction", *PNAS*, **100**:13910-13915 (2003).
12. E. Ben-Jacob, "Bacterial self-organization: co-enhancement of complexification and adaptability in a dynamic environment", *Phil. Trans. R. Soc. Lond. A*, **361**:1283-1312 (2003).
13. H.S. Yoon and J.W. Golden, "Heterocyst pattern formation controlled by a diffusible peptide", *Science*, **282**:935-938 (1998).
14. C. Zandonella, "The tiny toolkit", *Nature*, **423**:10-12 (2003).
15. Y.F. Dufrene, "Atomic Force Microscopy, a Powerful Tool in Microbiology", *J. Bact.*, **184**:5205-5213 (2002).
16. S.K. Jericho *et al.*, "MEMS microtweezers for the manipulation of bacteria and small particles", preprint (2003).
17. F. Gerbal *et al.*, "Measurement of the elasticity of the actin tail of *Listeria monocytogenes*", *Eur. Biophys. J.*, **29**:134-140 (2000).
18. H. Kitano, "Computational systems biology", *Nature*, **420**:206-210 (2002).
19. "Geomicrobiology: interactions between microbes and minerals", *Reviews in Mineralogy* vol. 35, eds. J.F. Banfield and K.H. Neals, MSA Press, 1997.
20. K. Edwards and A.D. Rutenberg, "Microbial response to surface microtopography", *Chem. Geol.*, **180**:19-32 (2001).
21. J.D. Klein *et al.*, "Direct measurement of interaction forces between a single bacterium and a flat plate", *J. Colloid and Interface Sci.*, **261**:379-385 (2003).
22. H. Morisaki, "Measurement of the force necessary for removal of bacterial cells from a quartz plate", *J. Gen. Microbiol.*, **137**: 2649-2655 (1991).
23. Y.-L. Ong *et al.*, "Adhesion forces between *E. coli* bacteria and biomaterial surfaces", *Langmuir*, **15**:2719-2725 (1999).
24. *Cellular Microbiology*, eds. P. Cossart, P. Boquet, S. Normark, and R. Rappuoli, ASM Press, 2000.
25. J.A. Theriot, "The cell biology of infection by intracellular bacterial pathogens", *Annu. Rev. Cell Dev. Biol.*, **11**:213-239 (1995); S. Dramsi and P. Cossart, "Intracellular pathogens and the actin cytoskeleton", *Annu. Rev. Cell Dev. Biol.*, **14**:137-166 (1998); RA. Heinzen *et al.*, "Dynamics of actin-based movement by *Rickettsia rickettsii* in Vero cells", *Infect. Immun.*, **67**:4201-4207 (1999); S. Cudmore *et al.*, "Actin-based motility of *Vaccinia virus*", *Nature*, **378**:636-638 (1995).
26. A. Mogilner and G. Oster, "Cell motility driven by actin polymerization", *Biophys. J.*, **71**:3030-3045 (1996); A. Mogilner and L. Edelstein-Keshet, "Regulation of actin dynamics in rapidly moving cells: a quantitative analysis", *Biophys. J.*, **83**:1237-1258 (2002).
27. A.D. Rutenberg and M. Grant, "Curved tails in polymerization-based bacterial motility", *Phys. Rev. E* **64**:21904 (2001).
28. A.D. Rutenberg, A.J. Richardson, and C.J. Montgomery, "Diffusion of asymmetric swimmers", *Phys. Rev. Lett.*, **91**:80601.1-4 (2003).
29. F. Perrin, "Mouvement Brownien d'un ellipsoïde", *J. de Physique et le Radium*, **5**:497 (1934).
30. J.R. Robbins and J.A. Theriot, "*Listeria monocytogenes* rotates around its long axis during actin-based motility", *Current biology*, **13**:R754-R756 (2003).
31. P.J. Flory, *Statistical mechanics of chain molecules*, Hanser Gardner, 1989.
32. M. Doi and S.F. Edwards, *The Theory of Polymer Dynamics*, Oxford, 1986.
33. W. Margolin, "Spatial regulation of cytokinesis in bacteria", *Current Opinion Microbiol.*, **4**:647-652 (2001).
34. D. M. Raskin and P. A. J. de Boer, "Rapid pole-to-pole oscillation of a protein required for directing division to the middle of *Escherichia coli*", *Proc. Natl. Acad. Sci. USA*, **96**:4971-4976 (1999).
35. D.M. Raskin and P.A.J. de Boer, *J. Bacteriol.*, **181**:6419-6424 (1999).
36. Z. Hu and J. Lutkenhaus, "Topological regulation of cell division in *Escherichia coli* involves rapid pole to pole oscillation of the division inhibitor MinC under the control of MinD and MinE", *Mol. Microbiol.* **34**:82-90 (1999).
37. C.A. Hale *et al.*, "Dynamic localization cycle of the cell division regulator MinE in *Escherichia coli*", *EMBO*, **20**:1563-1572 (2001).
38. M. Howard, A.D. Rutenberg, and S. de Vet, "Dynamic compartmentalization of bacteria: accurate division in *E. coli*", *Phys. Rev. Lett.*, **87**:278102 (2001).
39. Y.-L. Shih *et al.*, "Division site placement in *E.coli*: mutations that prevent formation of the MinE ring lead to loss of the normal midcell arrest of growth of polar MinD membrane domains", *EMBO*, **21**:3347-3357 (2002).
40. M. Howard and A.D. Rutenberg, "Pattern formation inside bacteria: fluctuations due to the low copy number of proteins", *Phys. Rev. Lett.*, **90**:128102.1-4 (2003).
41. X.-C. Yu and W. Margolin, "FtsZ ring clusters in min and partition mutants: role of both the Min system and the nucleoid in regulating FtsZ ring localization", *Mol. Microbiol.*, **32**:315-326 (1999).
42. H. Meinhardt and P.A.J. de Boer, "Pattern formation in *E. coli*: a model for the pole-to-pole oscillations of Min proteins and the localization of the division site", *PNAS*, **98**:14202-14207 (2001); K. Kruse, "A dynamic model for determining the middle of *E. coli*", *Biophys. J.*, **82**:618-627 (2002); K.C. Huang, Y. Meir, and N.S. Wingreen, "Dynamic structures in *Escherichia coli*: spontaneous formation of MinE rings and MinD polar zones", *PNAS*, **100**:12724-12728 (2003).
43. Y.-L. Shih, T. Le, and L. Rothfield, "Division site selection in *Escherichia coli* involves dynamic redistribution of Min proteins within coiled structures that extend between the two cell poles", *PNAS*, **100**:7865-7870 (2003).
44. U. Alon, "Biological networks: the tinkerer as an engineer", *Science*, **301**:1866-1867 (2003); N. Barkai and S. Leibler, "Robustness in simple biochemical networks", *Nature*, **387**:913-917 (1997).
45. C.V. Rao *et al.*, "Control, exploitation and tolerance of intracellular noise", *Nature*, **420**:231-237 (2002).